Knowledge-Guided Automatic Segmentation of the Left Ventricle from MR

A Pednekar[1], IA Kadadiaris[1], R Muthupillai[2], S Flamm[3]

[1]Visual Computing Lab, Dept. of Computer Science, Univ. of Houston, Houston, TX, USA
[2]Philips Medical Systems North America, Bothell, WA, USA
[3]Dept. of Radiology, St. Luke's Episcopal Hospital, Houston, TX, USA

Abstract

The routinely used clinical practice of manual tracing of the blood pool from short axis cine MR images to compute ejection fraction (EF) is cumbersome, time consuming, and operator dependent. In this paper, we present an algorithm that automatically segments the left ventricle (LV) using the a priori knowledge of the intensity responses of the tissue in different MR modalities, along with the LV morphology. Our method for the automatic computation of the EF is based on segmenting the left ventricle by combining the fuzzy connectedness and the physics-based deformable model frameworks. We have validated our method against manual delineation performed by experienced radiologists on the data from nine asymptomatic volunteers with very encouraging results.

1. Introduction

At present, in routine clinical practice, delineation of LV is performed manually on a large number of 3D cine MR images. In the hands of an experienced operator, this can be quite accurate; however, manual tracing is very subjective and can be very difficult for those new in the field, resulting in possible inaccuracies. Thus manual tracing of the endocardial boundary is labor-intensive, and time-consuming and involves considerable inter- and intra-observer variations [1]. These limitations have motivated the development of automated segmentation techniques for more accurate and more reproducible LV segmentation. Automation of LV segmentation poses challenges due to automatic localization of the LV in MR scans, the inherently fuzzy nature of cardiac MR due to heart dynamics, and the presence of papillary muscles inside the LV blood pool. Currently there is no known single method available which, can automatically localize the LV, segment the fuzzy MR with high accuracy without user interaction, and also take into account the presence of the papillary muscles in the LV. We have developed a hybrid segmentation approach for the automatic computation of the EF from dual contrast (balanced fast field echo - turbo spin echo) short axis cardiac MR data, which combines the fuzzy connectedness region-based segmentation method with the LV-specific elastically adaptive deformable model-based boundary segmentation method. Although we require an additional TSE scan at diastole, this can be performed in just a single additional breath-hold, and thus does not have any significant effect on the total scan time. Also, the slight inaccuracies in the 3D registration due to partial voluming do not affect the segmentation results, as dual contrast information is used only for the preliminary estimation of the LV region. We have compared our method's results for EF to manual delineation performed by experienced radiologists on the data from nine asymptomatic volunteers with very encouraging results. Our work is inspired by the work of Metaxas' and Udupa's research groups [2, 3, 4, 5]. Our enhancements and contributions are the following: 1) segmentation of multi-valued data as opposed to segmentation of scalar data is perfomrmed; 2) our algorithm does not need any manually selected seed area for the fuzzy connectedness; 3) we have automated the fuzzy connectedness method by determining the dynamic weights for the homogeneity and the gradient energy functions adaptively; 4) in our algorithm there is no iteration between the deformable model and the fuzzy connectedness algorithm; 5) we have developed a new class of forces derived from dual contrast and fuzzy connectedness data for physics-based deformable model, which is integrated with the customized model for the LV, by the addition of LV-specific shape constraints, thus eliminating user interaction at both the LV identification and the LV segmentation phases. The remainder of this paper describes our technique in detail. In the next section we explain the theoretical framework for our method. Section 3 details the implementation specifics, and we present the results in section 4. Finally we conclude the paper with a discussion of the merits of our method.

2. Theoretical framework

Before we explain our algorithm in detail, we review some concepts from the fuzzy connectedness and

Computers in Cardiology 2002;29:193–196.

the deformable model frameworks and we detail our extensions.

Adaptive Fuzzy Connectedness: The Fuzzy Connected Image Segmentation framework developed by Udupa and his collaborators [3, 6] assigns fuzzy affinities between two given pixels or voxels in an image or a volume based on a weighted function of the degree of coordinate space adjacency, degree of intensity space adjacency, and degree of intensity gradient space adjacency to the corresponding target object features. Specifically, the membership function of the fuzzy spel affinity is defined as: follows: $\mu_k(c,d) = \mu_\alpha(c,d)[\omega_1 h_1(I(c),I(d)) + \omega_2 h_2(I(c),I(d))]$, if $c \neq d$ and $\mu_k(c,c) = 1$, where $\mu_\alpha(c,d)$ is the membership function of the spatial adjacency between spels c and d, I denotes the intensity values, and ω_1 and ω_2 are free parameters satisfying: $\omega_1 + \omega_2 = 1$. For dual contrast neighborhood, we used functions as suggested in [3]: $h_1 = \frac{1}{(2\pi)^{\frac{n}{2}}|\mathbf{S}_1|^{\frac{1}{2}}} e^{-\frac{1}{2}[\frac{1}{2}(\mathbf{I}(c)+\mathbf{I}(d))-\mathbf{m}_1]^\top \mathbf{S}_1^{-1}[\frac{1}{2}(\mathbf{I}(c)+\mathbf{I}(d))-\mathbf{m}_1]}$ $h_2 = \frac{1}{(2\pi)^{\frac{n}{2}}|\mathbf{S}_2|^{\frac{1}{2}}} e^{-\frac{1}{2}[|\mathbf{I}(c)-\mathbf{I}(d)|-\mathbf{m}_2]^\top \mathbf{S}_2^{-1}[|\mathbf{I}(c)-\mathbf{I}(d)|-\mathbf{m}_2]}$ where $\mathbf{I}(c) = (I_{bFFE}(c), I_{TSE}(c))$ is the two component intensity vector, $\mathbf{m}_1$ and $\mathbf{S}_1$ are the mean vector and covariance matrix of spels in the intensity space, $\mathbf{m}_2$ and $\mathbf{S}_2$ are the mean vector and covariance matrix of spels in the gradient magnitude space. With ω_1 and ω_2 kept as free parameters, the results obtained from fuzzy connectedness remain highly sensitive to the selection of the sample region. To overcome this problem, we compute ω_1 and ω_2 as adaptive parameters depending on the ratio of homogeneity and gradient function values at each spel location: $\omega_1 = \frac{h_1}{(h_1+h_2)}$ and $\omega_2 = 1 - w_1$. This method of weight assignment takes advantage of the fact that when the spels are closer to the center of the target object, then the degree of intensity space adjacency will be higher than when a spel is near the boundary of the target. As a spel moves towards the boundary, automatically more weight is given to the degree of adjacency in intensity gradient space, thus enabling more accurate boundary definition. In particular, this method enhances the difference in affinities attached to the pixels on either side of the boundary, and thus gives better defined fuzzy objects without involving a user to adjust the values of these parameters to find the best possible combination of ω_1 and ω_2. To improve the accuracy of the boundary information, we incorporate information from both the imaging spectra to compute the fuzzy affinities. Since our refined fuzzy connectedness attaches much higher affinities to the target object relative to rest of the image, the need for complex algorithm to determine the appropriate threshold to segment the membership scene is eliminated. In addition, the edge magnitudes of fuzzy affinity images are pronounced which is crucial for the integration with the deformable model.

Deformable Model: To extract and reconstruct the LV surface from the 3D dual contrast MR data, we employ an elastically adaptive deformable model [2]. We have defined a new class of forces derived from multi-valued volume data that localize salient data features. In order to attract our model towards significant 3D gradients of the multi-spectral data $\mathbf{I}(x,y,z) = (I_{bFFE}(x,y,z), I_{TSE}(x,y,z))^\top$ and of the volume fuzzy connectedness data $\mathbf{F}$ derived with the techniques explained in the previous section, we construct a 3D potential function as follows: $\mathbf{P}(x,y,z) = \lambda_1||D_{MD} * \mathbf{I}|| + \lambda_2||D_{MD} * \mathbf{F}||$, whose potential minima coincides with the LV surface. The 3D Monga-Deriche (MD) operator is applied to the multi-valued data and the fuzzy connectedness data to produce two gradient fields. A weighted combination of these terms is formed to force the model to drop into the deeper valleys and lock onto the LV surface boundary. Then, the following force distribution can be derived from this potential function: $\mathbf{f}(x,y,z) = c\frac{\nabla \mathbf{P}(x,y,z)}{||\nabla \mathbf{P}(x,y,z)||}$, where the variable c controls the strength of the force. Once the model converges towards the LV boundary, the smoothing effect of the model will allow it to ignore the data from the papillary muscle. Computation of the forces at any model point is achieved using tri-linear interpolation.

3. Ejection fraction computation

Step 1 - Acquire and pre-process the data: Studies were performed in nine subjects (7m/2f) with normal sinus rhythm, with consent. Contiguous 10mm short axis slices were obtained to cover the left ventricle (LV) from the apex of the ventricle to the mitral valve annulus within a breath-hold. For this study, it was assumed that respiratory motion with the breath-hold would be negligible. Scans were acquired using a dual IR black-blood sequence (TE/TR/TSE factor: 80/2hb/23, a single diastolic phase), and cine bFFE sequence (TE/TR/flip: 3.2/1.6/55 deg; 38-40 msec temporal resolution) using VCG gating at 1.5T. A TSE scan can be performed in just a single additional breath-hold and thus does not have any significant effect on the total scan time. All the images were stored in standard DICOM format. Figs. 1(a,b) depict the data from the 6th bFFE and TSE slice (subject-1). The data were analyzed manually by experienced radiologists and using the automated analysis in a post-processing workstation. 3D registration of the diastolic bFFE and TSE volumes is achieved using the Normalized Mutual Information algorithm.

Step 2 - Construct spatio-dual-intensity 4D vector space: The promise of dual contrast acquisition is that the dimensionally expanded measurement space will allow differentiations about the different tissues to be made, which are impossible in any of the component images. To

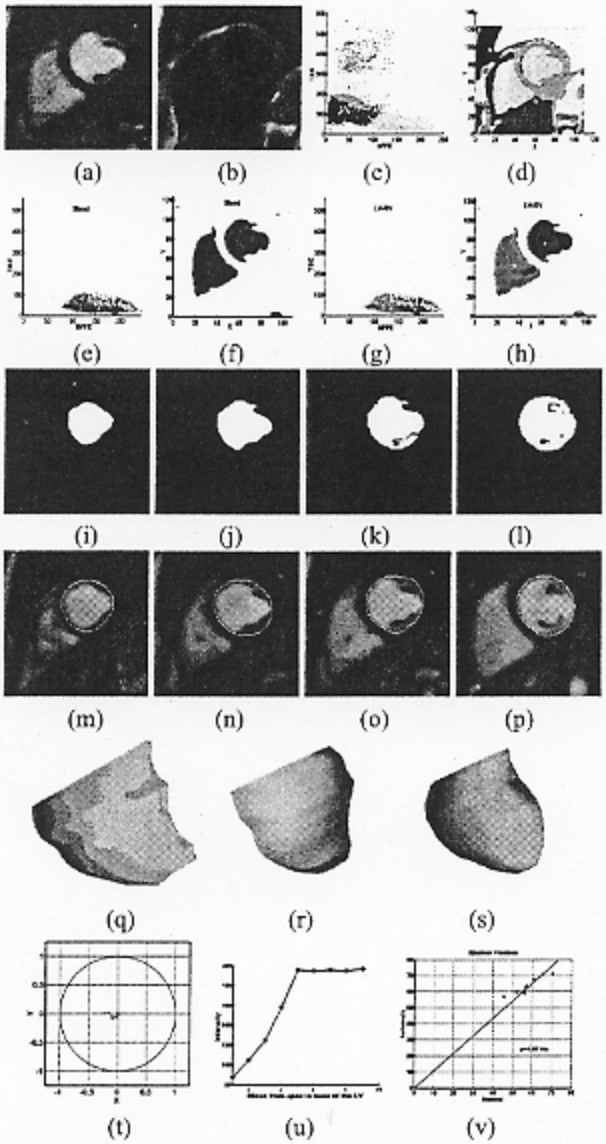

Figure 1. (a,b) Slice 6 from the bFFE and TSE scans of Subject-1. (c) Projection of the 4D measurement space on bFFE-TSE, and (d) x-y planes, respectively. Projection of the identified blood cluster on the (e) TSE-bFFE and (f) x-y planes, respectively. Projection of the identified LV and RV clusters and centroids on the (g) TSE-bFFE and (h) x-y planes, respectively. (i-l) Resulting fuzzy connectedness data. (m-p) Projection of the fitted elastically adaptive deformable model. Fitted deformable models of the LV blood pool for (q) Subject-1, (r) Subject-4, and (s) Subject-9 respectively. (t) Estimated centroids for nine subjects mapped on normalized circle fitted to the LVs obtained manually, (u) Coil intensity fall off in MR, and (v) EFs for nine subjects using the manual and the automatic method.

that end, we construct a four dimensional measurement space, which combines the spatial and dual contrast intensity information. The basis components of our 4D vector are the (x,y) Euclidean coordinates of the pixels and their signal intensities in bFFE and TSE scans. Tissue types due to their signal intensity responses (Fig 1(c)) and organs due to their spatial adjacency (Fig 1(d)) form 4D clusters in this measurement space, thus providing clues for tissue and organ classification.

Step 3 - Estimate the cluster center and the corresponding region for the LV: The three major tissue types present in the MR scans are blood, myocardium, and fat. For example in Fig. 1(c), we do observe a distinct cluster for blood, a number of clusters where myocardium cluster is expected, and a cluster due to background. In this specific case, fat being almost negligible doesn't appear as a distinct cluster. We employ a conventional Fuzzy C-means clustering to estimate these clusters. Having identified the blood cluster (Fig. 1(e)) we can easily classify the blood in the scan (Fig. 1(f)) as the projection of the blood cluster on the spatial (x-y) plane. The fact that LV blood appears brighter compared to RV blood in the bFFE, is used to split the blood cluster into two clusters - one for the LV and one for the RV (Fig. 1(g)). The cluster to the right on the bFFE-TSE plane corresponds to the LV. Projections of these clusters on spatial (x-y) plane give centroids and regions for LV and RV (Fig. 1(h)). Once the LV is identified this estimation is further rectified by using region growing to keep only the LV region and then we recompute its centroid. Fig. 1(t) depicts the estimated centroids for nine subjects mapped on a normalized circle fitted to the LVs. Note that the LVs of all the nine subjects were identified correctly with the estimated centroids always well within the LV blood pool.

Step 4 - Perform Fuzzy Connected LV blood pool segmentation: The estimated LV centroid and region are used as seed and sample statistics for our 3D adaptive dual contrast fuzzy connectedness algorithm. The average intensity of the LV blood pool drops off as we move towards the apex of the heart, due to coil intensity fall off (Fig. 1(u)). We start off with the central slice FCM-based LV estimation and perform segmenation of the central slice; then we use the same statistics for the next slice and update the seed (centroid), the threshold of the membership scene, and the intensity and gradient statistics to refine the segmentation. The new threshold for scene membership is computed as:

$$expoI = \frac{(prevSliceMeanLVInt - currSliceMeanLVInt)}{prevSliceMeanLVIntensity},$$

$$thresh = thresh \times e^{-\sqrt{expoI}}.$$

In this way, we adaptively propagate the LV blood pool segmentation along the volume and time.

Step 5 - Fit a Deformable Model: An elastically adaptive LV deformable model[2] is fitted to the fuzzy connectedness and dual contrast data using shape

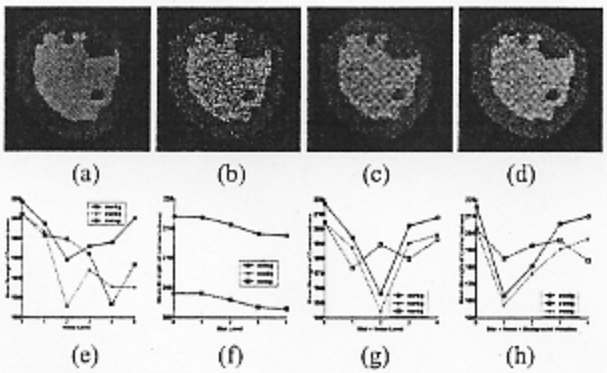

Figure 2. Images from phantom data set (a) plain synthetic image and images containing the following parameters: (b) noise, (c) blur + noise and,(d) blur + noise + background variation. Plots (e-h) depict results of comparitive study between adaptive and conventional fuzzy connectedness with $w_1 = w_2 = 0.5$ for various levels (g) blur, (h) noise, (i) blur plus noise, and (j) blur and noise plus background variation.

constraints. The domain specific prior knowledge that LV boundary is non-intersecting, closed and includes the papillary is incorporated to optimize fitting of deformable model to LV boundary (Fig. 1(q-s)). The elasticity parameters of the deformable model are changed adaptively depending on the gradient values allowing us to overcome spurious boundaries.

Step 6 - Compute the EF: Compute the ejection fraction (ratio of stroke volume to diastolic volume) by computing the volumes of the fitted deformable models at the end of systolic and diastolic phase.

4. Results, discussion and conclusion

We have performed a number of experiments to assess the accuracy, limitations and advantages of our approach.

For the first experiment, we designed synthetic 3D dual contrast datasets with different levels of noise, blurring, and gradual intensity change effects (Fig. 2), in order to assess the benefits from adapting the weights for fuzzy connectedness dynamically.

We use the mean values of strength of connectedness attatched to the ground truth as metric to compare the performace of adaptive fuzzy connectedness-based segmentation with respect to the conventional fuzzy connectedness-based segmentation. Fig. 2 shows the results of comparison study of the two methods on phantom dataset.

Next, we present the results from the segmentation of the data acquired from Subject-1. The segmentation results using adaptively weighted Fuzzy Connectedness for the LV blood pool are shown in Fig. 1(i-l). Figs. 1(m-p) depict projections of the fitted elastically adaptive shape-constrained deformable model on the corresponding slices. Figs. 1(q-s) depict the fitted deformable models for subjects 1, 4, and 9, respectively.

The EFs computed for nine volunteers using the manual method and automated blood segmentation method are shown in Fig. 1(y). Our initial validation results demonstrate the feasibility of using bFFE/TSE as multi-spectral data source to generate information necessary for automated segmentation of the LV.

The results show a slight overestimation of the EF using the automated technique. This is due to lack accuracy in apical slice segmentation, we expect to overcome this by incorporating inforamtion from long axis views. This justifies the use of deformable model as a last step to eliminate such spurious boundaries.

References

[1] Matheijssen N, Baur L, Reiber J, Van der Velde E, Van Dijkman P, Van der Geest R, de Ross A, Van der Wall E. Assessment of left ventricular volume and mass by cine magnetic resonance imaging in patients with anterior myocardial infarction: Intra-observer and inter-observer variability on contour detection. International Journal of Cardiac Imaging 1996;12:11–19.

[2] Metaxas D, Kakadiaris IA. Elastically adaptive deformable models. IEEE Transactions on Pattern Analysis and Machine Intelligence October 2002;(In press).

[3] Udupa J, Samarasekera S. Fuzzy connectedness and object definition: theory, algorithms, and applications in image segmentation. Graphical Models and Image Processing 1996; 58(3):246–261.

[4] Jones T, Metaxas D. Automated 3D segmentation using deformable models and fuzzy affinity. In Duncan J, Gindi G (eds.), Proceedings of the XVth International Conference on Image Processing in Medical Imaging, volume 1230. Poultney, Vermont: Springer, 1997; 113–126.

[5] Imielinska C, Metaxas D, Udupa J, Jin Y, Chen T. Hybrid segmentation of anatomical data. In MICCAI. 2001; .

[6] Saha P, Udupa J. Fuzzy connected object delineation: Axiomatic path strength definition and the case of mulitiple seeds. Computer Vision and Image Understanding 2001; 83:275–295.

Address for correspondence:

Ioannis A. Kakadiaris
Department of Computer Science
University of Houston
219 PGH, MS CSC 3010
Houston, TX 77204-3010, USA
tel./fax: +1-713-743-1255/1250
ioannisk@uh.edu